Appendix table of content

Appendix Figure S1 Effect of normoxia, physioxia and hypoxia on osteoclastogenesis. (A) Bone marrow cells were cultured with 10 ng/ml M-CSF under atmospheric air in a humidified incubator and then with 50 ng/ml RANKL in the presence of 10 ng/ml M-CSF under atmospheric air or 10% oxygen for 3 days. TRAP-stained cells (left panel) and the number of TRAP-positive cells with more than three nuclei (right). Scale bar, 100 μm. Data denote mean ± s.e.m. $^{**}P < 0.01$ (n = 3 biological replicates; t-test). (B) BMMs were cultured with M-CSF and RANKL in the presence of 10 nM 1,25-dihydroxyvitamin D_3, 100 nM prostaglandin E_2 and 10 nM dexamethasone under 5%, 2% and 1% oxygen for 4 days. TRAP-stained cells (left panel) and the number of TRAP-positive cells with more than three nuclei (right). These results were similar to those from a previous study(Fukuoka *et al*., 2005), but were contrary to those from a study wherein the cells were cultured on ivory discs, which showed that changing the oxygen concentration from 5% to 2% promoted osteoclast formation(Arnett *et al*., 2003). However, since the study showed that changing the oxygen concentration from 2% to 0.2% inhibited osteoclast formation, the ivory discs could be responsible for causing the shift in oxygen concentration threshold to attenuate osteoclast formation. Scale bar, 100 μm. Data denote mean ± s.e.m. $^{**}P < 0.01$ (n = 3 biological replicates; ANOVA). (C, D) Percentage of BrdU-labeled $CD11b^+$ BMMs (C) and Annexin V^+ $CD11b^+$ BMMs (D) cultured in 5% and 2% oxygen. Data denote mean ± s.e.m. NS, not significant (n = 3 biological replicates; t-test).

Appendix FIgure S1

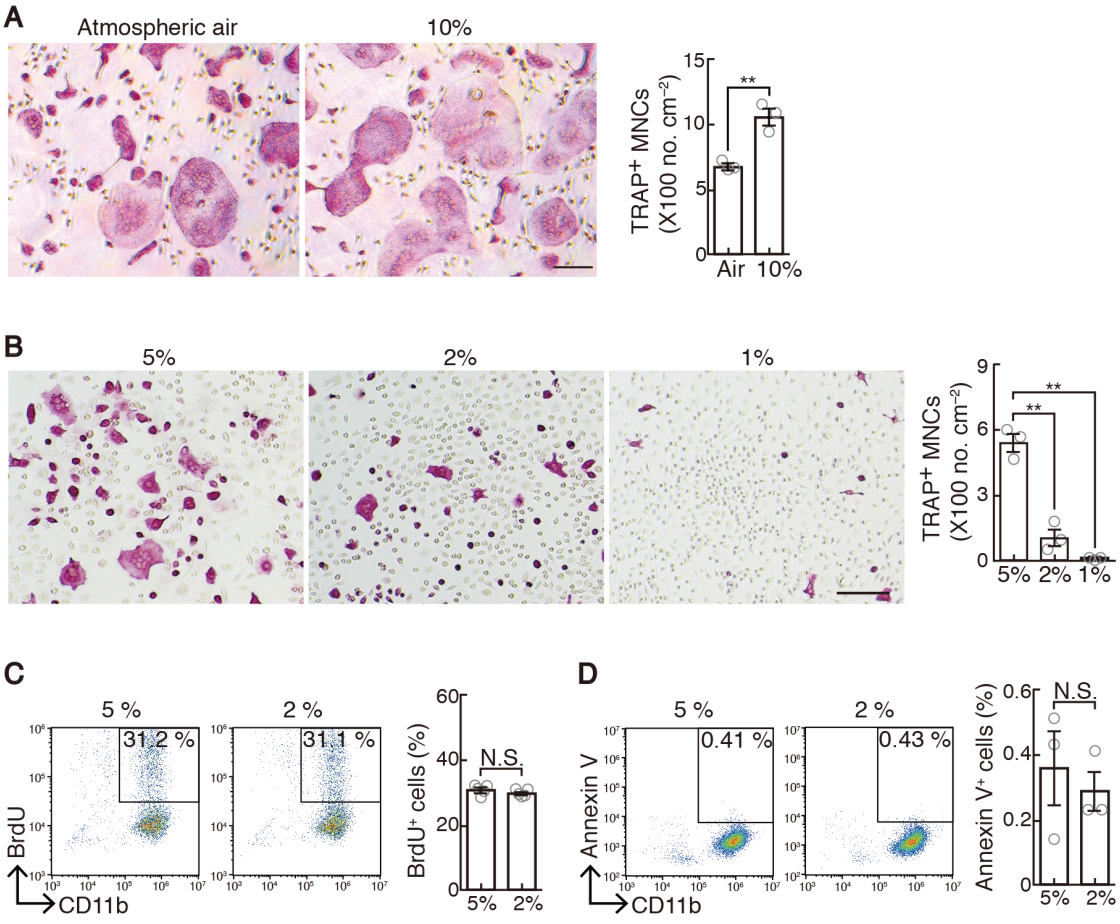

Appendix Figure S2 Expression of *Hif-1a*, *Hif-2a*, *Arnt*, *Vhl*, *Phds*, ten-eleven translocation (TET), lysine demethylase (KDM), nucleotide hydroxylase, collagen prolyl hydroxylase and prolyl hydroxylase families during osteoclast differentiation.

Bone marrow cells were cultured with 10 ng/ml M-CSF and then cultured with 50 ng/ml RANKL in the presence of 10 ng/ml M-CSF for 3 days. Total RNA was extracted from the cells 0, 24 and 72 h after RANKL stimulation and was then converted into cDNA by reverse transcription. Biotinylated cRNA was then synthesized by *in vitro* transcription. After cRNA fragmentation, hybridization with the mouse genome 430 2.0 array (Affymetrix) was performed. The data set has been deposited in the Genome Network Platform (http://genomenetwork.nig.ac.jp/). GeneChip analysis of *Hif-1a*, *Hif-2a*, *Arnt*, *Vhl* and *Phds* mRNA (A) (n = 1), and mRNA encoding for ten-eleven translocation enzyme (TET), lysine demethylase (KDM), nucleotide hydroxylase, collagen prolyl hydroxylase and prolyl hydroxylase families (B) (n = 1).

Appendix FIgure S2

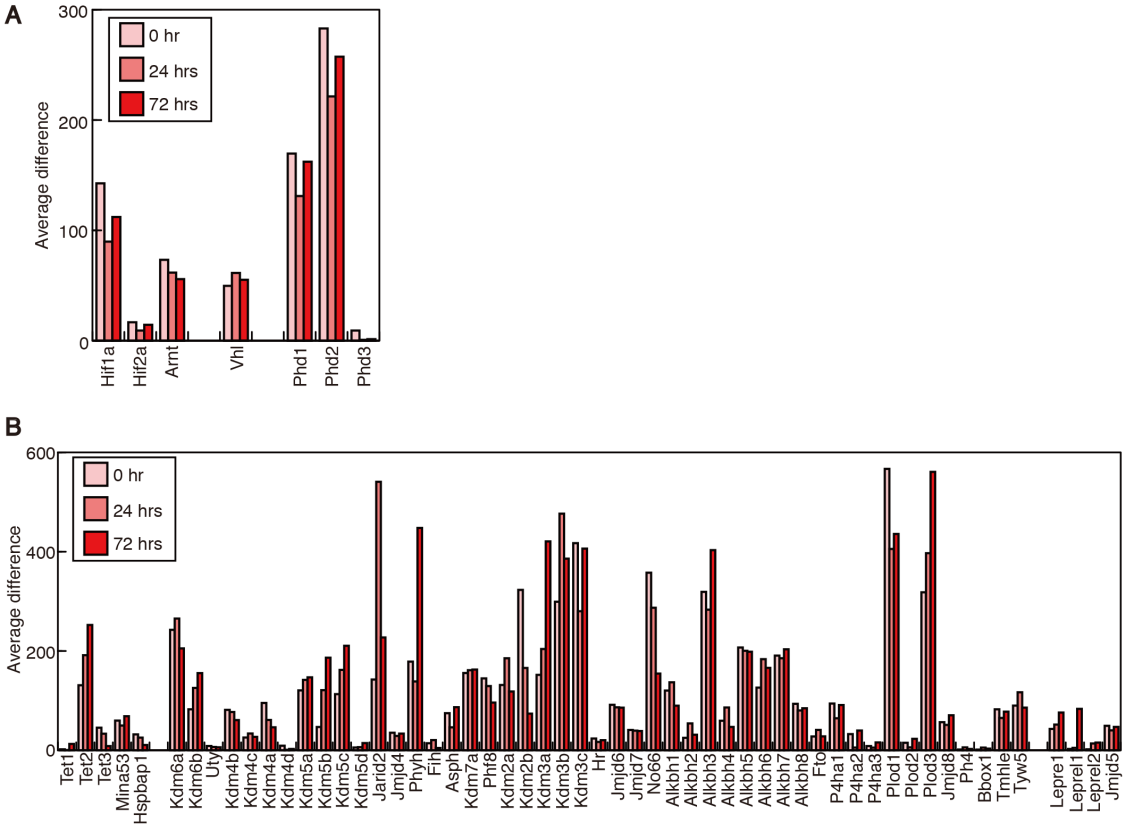

Appendix Figure S3 Enzymatic activity of iron (II)- and 2-oxoglutarate-dependent dioxygenases.

The K_M values for oxygen in hydroxylation reaction by dioxygenases were determined as previously described(Hancock *et al*, 2017; Hirsila *et al*., 2003; Koivunen *et al*, 2004; Laukka *et al*., 2016).

Appendix FIgure S3

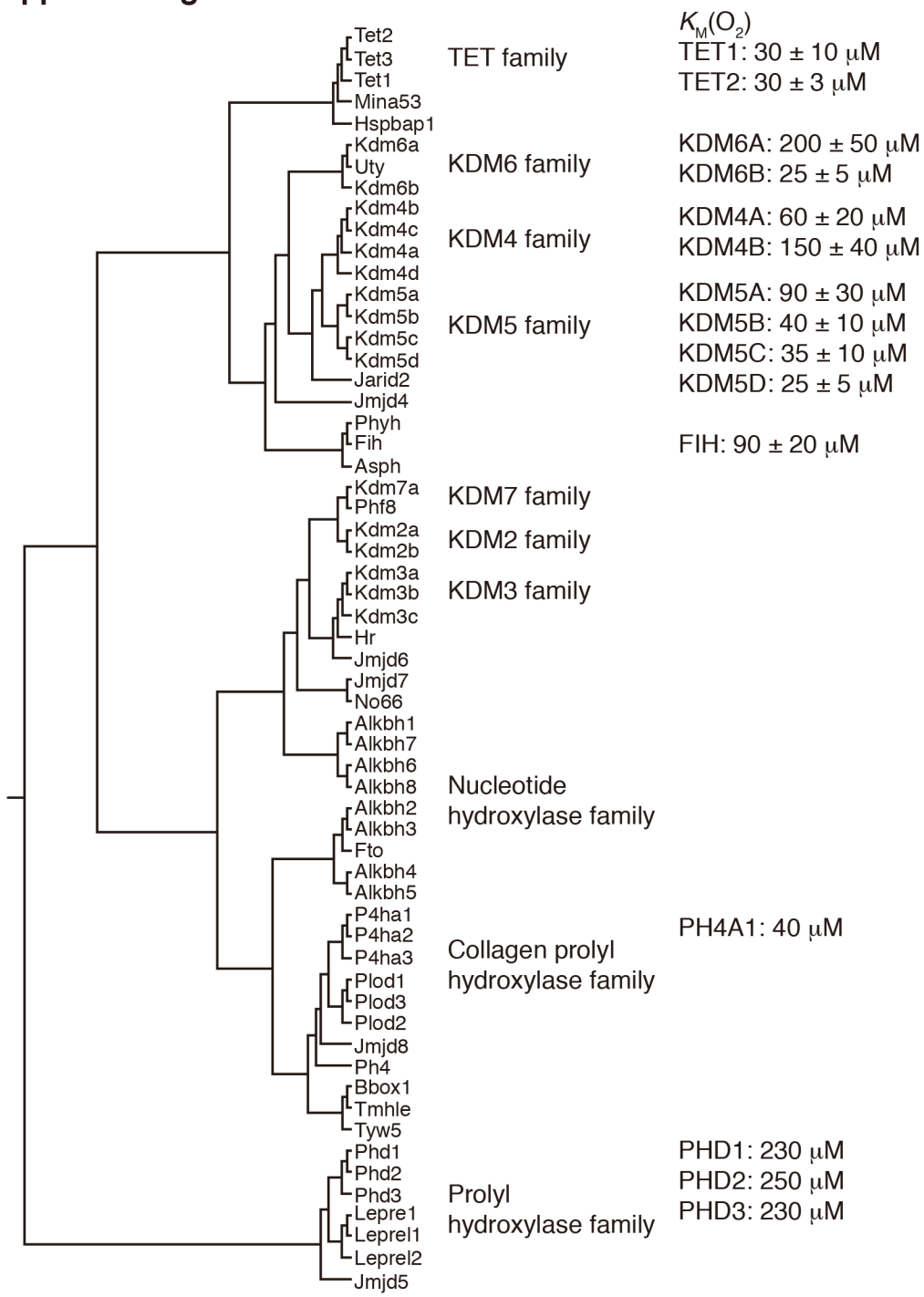

Appendix Figure S4 A plot of the difference in the reaction rate between pO_2 of 36.9 and 17.4 mmHg as a function of the Km values for oxygen in hydroxylation reaction by dioxygenases that obeys Michaelis-Menten kinetics (n = 1).

Appendix FIgure S4

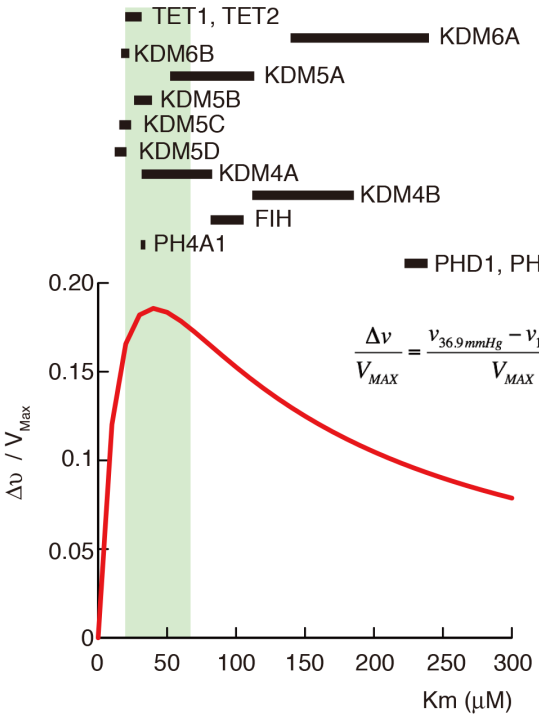

$$\frac{\Delta v}{V_{MAX}} = \frac{v_{36.9mmHg} - v_{17.4mmHg}}{V_{MAX}} = \frac{pO_2(36.8mmHg)}{Km + pO_2(36.8mmHg)} - \frac{pO_2(17.4mmHg)}{Km + pO_2(17.4mmHg)}$$

Appendix Figure S5 Effect of physiological hypoxia on histone modifications and DNA methylation.

(A) Methylation of histone H3 in BMMs stimulated with RANKL and cultured under 5% and 2% oxygen for 3 days. (B) DNA methylation in BMMs stimulated with RANKL and cultured under 5% and 2% oxygen for 3 days. Dot blot assay was performed using anti-5mC antibody (Left). Ethidium bromide staining was used to monitor equivalent DNA loading (right).

Appendix FIgure S5

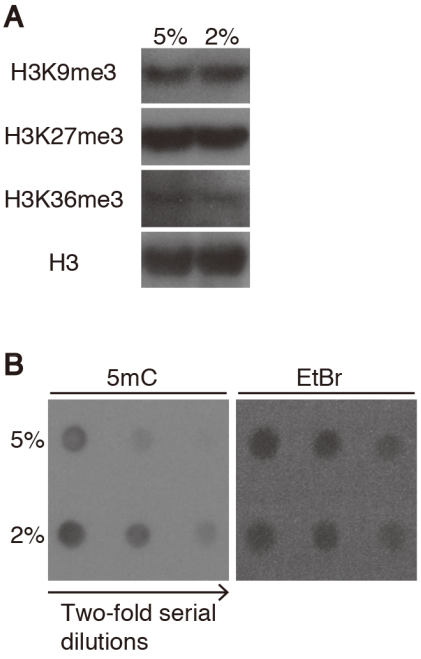

Appendix Figure S6 Bone phenotype of osteoclast-specific *Tet2*- and *Tet3*-deficient mice.

μCT analysis of the femurs of 10-week-old control (n = 3) and $Tet2_{CX3CR1}^{-/-}$; $Tet3a_{CX3CR1}^{-/-}$ (n = 3) male mice (left top panel: longitudinal view; left bottom panel: axial view of the metaphyseal region). Scale, 0.5 mm. Data denote mean ± s.e.m. $^{**}P < 0.01$ (n = 5 (control) and n = 3 ($Tet2_{CX3CR1}^{-/-}$; $Tet3a_{CX3CR1}^{-/-}$) biological replicates; t-test).

Appendix FIgure S6

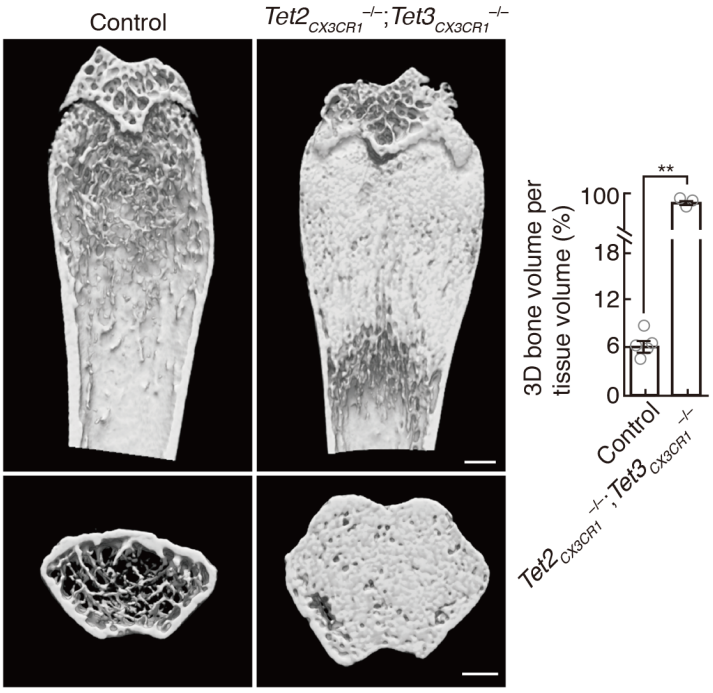

Appendix Figure S7 Effect of *Tet2* and *Tet3* deficiency on osteoclastogenesis.

(A) Expression of osteoclastogenic genes in wild-type control and $Tet2_{Rank}^{-/-}$; $Tet3a_{Rank}^{+/-}$ BMMs stimulated with RANKL. Data denote mean ± s.e.m. $^{**}P < 0.01$ (n = 4 biological replicates; t-test). (B) Effect of TETs overexpression on osteoclastogenesis of wild-type control and $Tet2_{Rank}^{-/-}$; $Tet3a_{Rank}^{+/-}$ BMMs stimulated with RANKL. For overexpression of TET derivatives, RNA transfection was performed with the Lipofectamine MessengerMAX according to the manufacturer's instructions. Synthetic capped RNA was prepared with the mMESSAGE mMACHINE T7 ULTRA Transcription kit using linearized DNA of the pcDNA3-FLAG-tagged TET derivatives and then purified using the RNeasy Mini kit. Two hours after transfection with RNA, BMMs were cultured with 50 ng/ml RANKL in the presence of 10 ng/ml M-CSF for 3 days. TRAP-stained cells (left panel), the number of TRAP-positive cells with more than three nuclei (upper right) and the expression of exogenous TET proteins (lower right). Scale bar, 100 μm. Data denote mean ± s.e.m. $^{**}P < 0.01$; NS, not significant (n = 4 biological replicates; ANOVA).

Appendix Figure S7

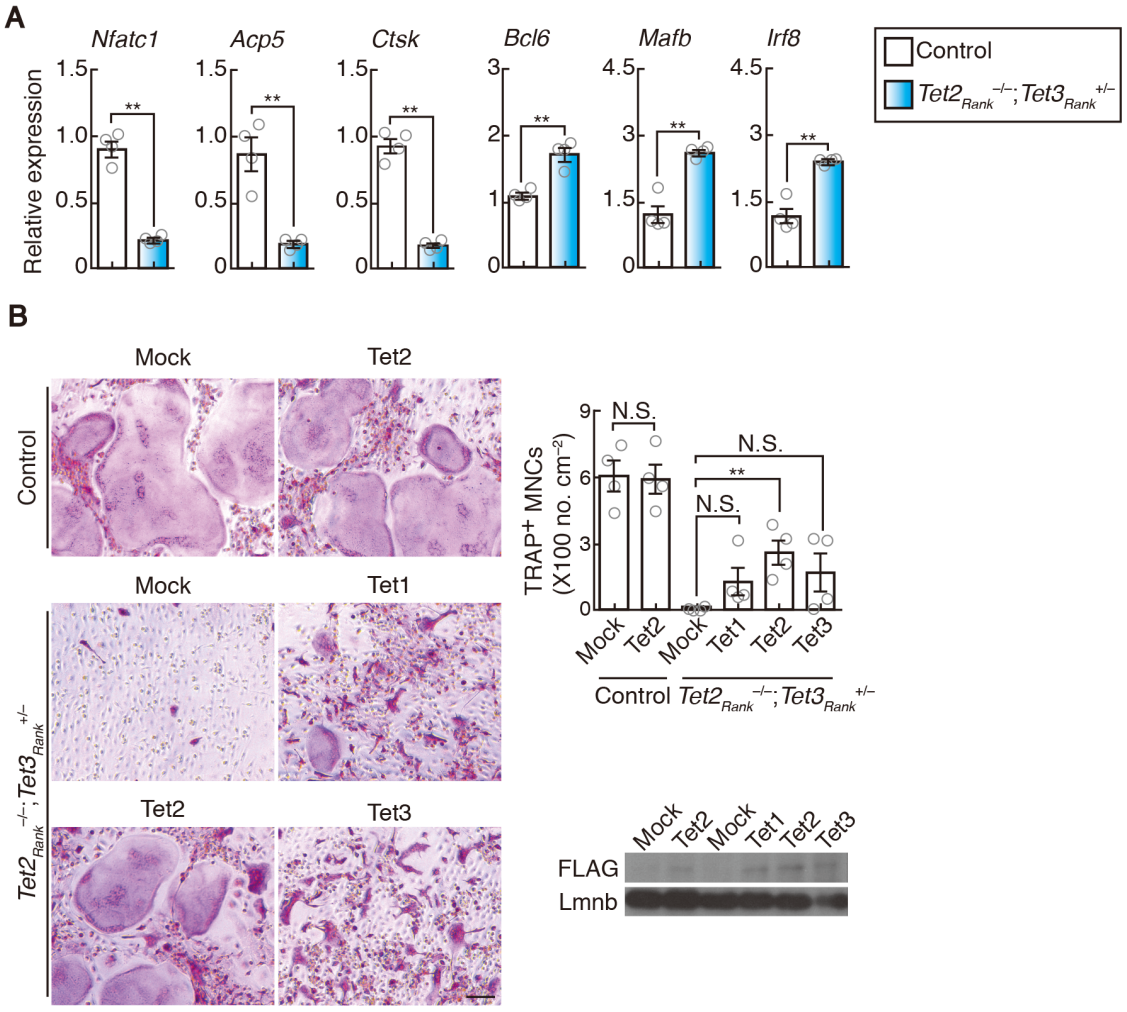

Appendix Figure S8 Effect of a broad-spectrum inhibitor of 2-oxoglutarate-dependent oxygenase, IOX1, and a TET-specific inhibitor, Octyl-2-hydroxyglutarate (2HG) on cell proliferation, survival and differentiation.

(A) Effect of IOX1 and 2-HG on osteoclast formation. Scale bar, 100 μm. Data denote mean ± s.e.m. $^{**}P < 0.01$; NS, not significant (n = 3 biological replicates; ANOVA). (B) Effect of IOX1 and 2-HG on the expression of osteoclatogenic genes. Data denote mean ± s.e.m. $^{**}P < 0.01$; NS, not significant (n = 3 biological replicates; ANOVA). (C, D) Percentage of BrdU-labeled $CD11b^+$ BMMs (C) and Annexin V^+ $CD11b^+$ BMMs (D) treated with 50 μM IOX1 or 100 μM 2HG. Data denote mean ± s.e.m. NS, not significant (n = 3 biological replicates; ANOVA).

Appendix FIgure S8

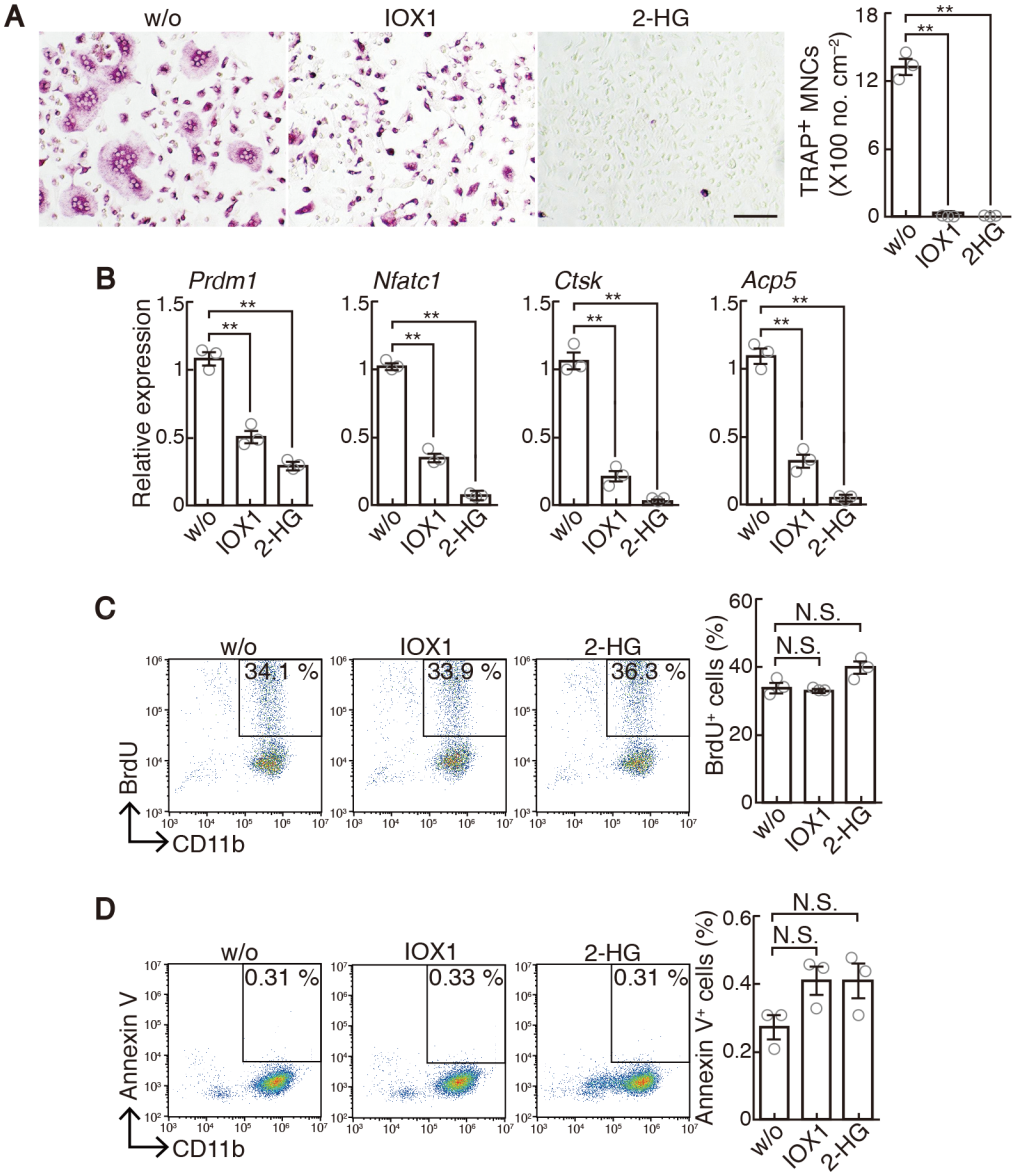

Appendix Figure S9 Effect of NFATc1 overexpression on osteoclastogenesis.

(A) MeDIP-qPCR analysis to validate regions that are hypermethylated in $Tet2_{Rank}^{-/-}$; $Tet3a_{Rank}^{+/-}$ BMMs stimulated with RANKL for 2 days. Data denote mean ± s.e.m. $*P < 0.05$ (n = 3-4 biological replicates; t-test). (B) Gene expression of TET target candidates in BMMs stimulated with RANKL for 2 days. Data denote mean ± s.e.m. $**P < 0.01$ (n = 7 biological replicates; t-test). (C) Protein expression of exogenous NFATc1 in control and $Tet2_{Rank}^{-/-}$; $Tet3a_{Rank}^{+/-}$ BMMs stimulated with RANKL for 2 days. (D) Effect of NFATc1 overexpression on osteoclast formation from untreated BMMs or BMMs treated with IOX1 or 2HG. TRAP-stained cells (left panel), protein expression of exogenous NFATc1 (upper right) and the number of TRAP-positive cells with more than three nuclei (lower right). Scale bar, 100 μm. Data denote mean ± s.e.m. $*P < 0.05$; $**P < 0.01$ (n = 3 biological replicates; t-test). (E) Protein expression of exogenous NFATc1 in BMMs stimulated with RANKL for 2 days under 5% and 2% oxygen.

Appendix FIgure S9

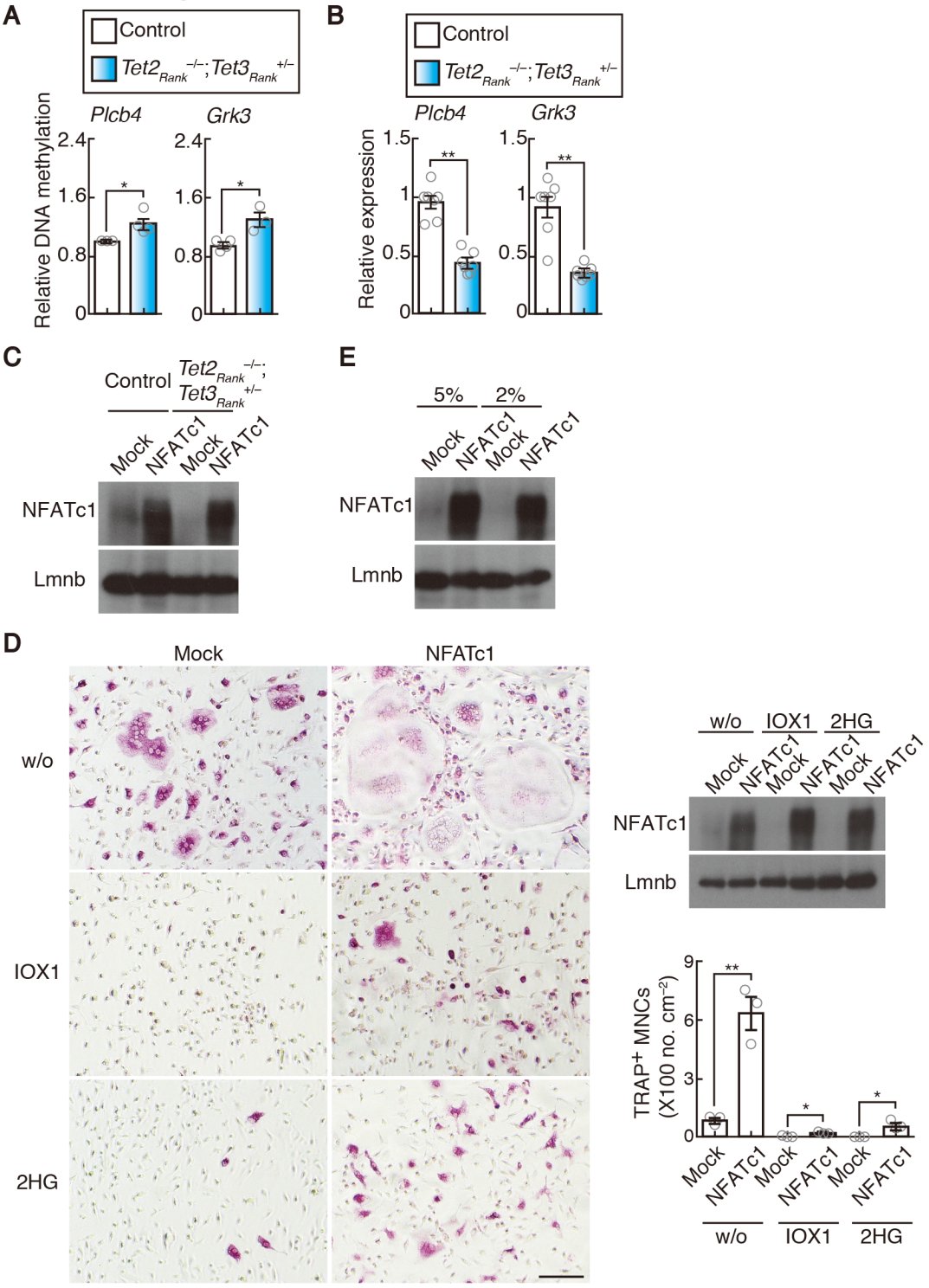

Appendix table S1

A list of primers used for quantitative RT-PCR analysis

Gene Symbol	Sequence
Actb	5’-CTTCTACAATGAGCTGCGTG-3’
	5’-TCATGAGGTAGTCTGTCAGG-3’
Tet1	5’-TGCACCTACTGCAAGAATCG-3’
	5’-TTTGGGCTTCTTTTCCCTCT-3’
Tet2	5’-ACATGCCAAATGGCAGTACA-3’
	5’-CCGCTTTCTTCTTGCAACTC-3’
Tet3	5’-CACTGAAGTTGCTCCCCTCT-3’
	5’-AAGGGTCTCCCTTCCTTCAG-3’
Irf8	5’-GGAAAGCCTTACCTGCTGAC-3’
	5’-AAGGTCACCGTGGTCCTTAG-3’
Mafb	5’-TCCACCTCTTGCTACGTGTG-3’
	5’-CGTTAGTTGCCAATGTGTGG-3’
Bcl6	5’-CCGGCACGCTAGTGATGTT-3’
	5’-TGTCTTATGGGCTCTAAACTGCT-3’
Nfatc1	5’-GGTAACTCTGTCTTTCTAACCTTAAGCTC-3’
	5’-GTGATGACCCCAGCATGCACCAGTCACAG-3’
Actp5	5’-GGGAAATGGCCAATGCCAAAGAGA-3’
	5’-TCGCACAGAGGGATCCATGAAGTT-3’
Ctsk	5’-AGGCAGCTAAATGCAGAGGGTACA-3’
	5’-ATGCCGCAGGCGTTGTTCTTATTC-3’
Nfkb1	5’-ATGGCAGACGATGATCCCTAC-3’
	5’-TGTTGACAGTGGTATTTCTGGTG-3’
Nfkb2	5’-GGCCGGAAGACCTATCCTACT-3’
	5’-CTACAGACACAGCGCACACT-3’
Relb	5’-CCGTACCTGGTCATCACAGAG-3’
	5’-CAGTCTCGAAGCTCGATGGC-3’
Csf1r	5’-TGTCATCGAGCCTAGTGGC-3’
	5’-CGGGAGATTCAGGGTCCAAG-3’
Tnfsf11	5’-GGACGGTGTTGCAGCAGAT-3’
	5’-GCAGTCTGAGTTCCAGTGGTA-3’
Slc2a1	5’-CAGTTCGGCTATAACACTGGTG-3’
	5’-GCCCCCGACAGAGAAGATG-3’
Pkm2	5’-GCCGCCTGGACATTGACTC-3’
	5’-CCATGAGAGAAATTCAGCCGAG-3’
Hk1	5’-AGGGCGCATTACTCCAGAG-3’
	5’-CCCTGTGGGTGTCTTGTGTG-3’
Bnip3	5’-TCCTGGGTAGAACTGCACTTC-3’
	5’-GCTGGGCATCCAACAGTATTT-3’
Gapdh	5’-AGGTCGGTGTGAACGGATTTG-3’
	5’-TGTAGACCATGTAGTTGAGGTCA-3’

A list of primers used for quantitative RT-PCR analysis (continued)

Gene Symbol	Sequence
Prdm1	5'-TGCTTATCCCAGCACCCC-3'
	5'-CTTCAGGTTGGAGAGCTGACC-3'
Prkch	5'-TCCGGCACGATGAAGTTCAAT-3'
	5'-TACGCTCACCGTCAGGTAGG-3'
Plcb4	5'-GGACAAGTGCTAGAATGTTCCC-3'
	5'-GAAGCCGATATTCACCAGATCC-3'
Gsap	5'-CTCCCGAGTCTGCTCACAC-3'
	5'-CACGTAAGCTCCCATAAGTTGTT-3'
Scd2	5'-GCATTTGGGAGCCTTGTACG-3'
	5'-AGCCGTGCCTTGTATGTTCTG-3'
Grk3	5'-GTGTGTGCGCGATACATTGC-3'
	5'-GGGCTACATACCCCAGAGATAC-3'
Hif1a	5'-TCTCGGCGAAGCAAAGAGTC-3'
	5'-AGCCATCTAGGGCTTTCAGATAA-3'
Hif2a	5'-GAGGAAGGAGAAATCCCGTGA-3'
	5'-TATGTGTCCGAAGGAAGCTGA-3'

A list of primers used for methylated DNA immunoprecipitation analysis

Prdm1	5'-CCCCGGGACTATTTCAGTTT-3'
	5'-GCCTCCACAGTTAGCCGTAA-3'
Prkch	5'-GTAACTCATGTTTAAATCTCTCACG-3'
	5'-GATCACAGTCAACTCCCTGCAACAC-3'
Plcb4	5'-CGTAACCCATCTCAGCTTATCATTCA-3'
	5'-AGATGAGTGTTATCCTTCCGTTAAC-3'
Gsap	5'-CGAGTTAATTTTTTCCCCCTGAGGCG-3'
	5'-CTCTTCTTCTGAACAGGAAACGTCC-3'
Scd2	5'-AAATGAAGGTGAAAGACAGAAGG-3'
	5'-GGAAGCCCTGAGGAGTTCTGGGCC-3'
Grk3	5'-CTAAAGAGAATGACTATCTAAAAAC-3'
	5'-TGATTCTCCTGCCTCCGCCTCATAC-3'

A list of primers used for bisulfate sequencing analysis

Prdm1 2nd intron_NEST	5'-GAGTTAGTTATTAGAAAGTAGTT-3'
	5'-ATCAAACTCTAAAATAACAAAC-3'
Prdm1 2nd intron	5'-CAGTGTGCTGGAATTCAGTTTTAGTATTTGGATGATTGTAAA-3'
	5'-GATATCTGCAGAATTCAAACTATCAATTAATAACCCAACAC-3'

References

Fukuoka H, Aoyama M, Miyazawa K, Asai K, Goto S (2005) Hypoxic stress enhances osteoclast differentiation via increasing IGF2 production by non-osteoclastic cells. *Biochem Biophys Res Commun* 328: 885-894

Arnett TR, Gibbons DC, Utting JC, Orriss IR, Hoebertz A, Rosendaal M, Meghji S (2003) Hypoxia is a major stimulator of osteoclast formation and bone resorption. *J Cell Physiol* 196: 2-8

Hancock RL, Masson N, Dunne K, Flashman E, Kawamura A (2017) The Activity of JmjC Histone Lysine Demethylase KDM4A is Highly Sensitive to Oxygen Concentrations. *ACS Chem Biol* 12: 1011-1019

Hirsila M, Koivunen P, Gunzler V, Kivirikko KI, Myllyharju J (2003) Characterization of the human prolyl 4-hydroxylases that modify the hypoxia-inducible factor. *J Biol Chem* 278: 30772-30780

Koivunen P, Hirsila M, Gunzler V, Kivirikko KI, Myllyharju J (2004) Catalytic properties of the asparaginyl hydroxylase (FIH) in the oxygen sensing pathway are distinct from those of its prolyl 4-hydroxylases. *J Biol Chem* 279: 9899-9904

Laukka T, Mariani CJ, Ihantola T, Cao JZ, Hokkanen J, Kaelin WG, Jr., Godley LA, Koivunen P (2016) Fumarate and Succinate Regulate Expression of Hypoxia-inducible Genes via TET Enzymes. *J Biol Chem* 291: 4256-4265